On the origin of the saddle in the spectrum of holes in a CuO_2 plane

A. F. Barabanov, V. M. Berezovskiĭ, and É. Zhasinas

Institute of High-Pressure Physics, Russian Academy of Sciences, 142092 Troitsk, Moscow Region, Russia

L. A. Maksimov

Kurchatov Institute Russian Research Center, Institute of Superconductivity and Solid State Physics, 123182 Moscow, Russia

(Submitted 29 March 1996)
Zh. Éksp. Teor. Fiz. **110**, 1480–1496 (October 1996)

Using the effective hole Hamiltonian of Emery's three-band model for CuO_2 planes in high-T_c superconductors, we have calculated the spectrum of magnetic-polaron hole excitations. The resulting spectrum has been investigated as a function of frustration in the copper magnetic subsystem, the amplitude of direct hopping between oxygen atoms, temperature, and some other parameters of the model. Our calculations yield features of the spectrum observed in experiments, namely (1) an extended saddle-like region and (2) isotropic bottom of the band.
 [S1063-7761(96)02410-9]

1. INTRODUCTION

An important issue in developing a microscopic theory of high-T_c superconductivity is the dielectric function $\varepsilon(\mathbf{k})$ of hole excitations in the CuO_2 plane. Recent photoemission measurements with angular resolution indicate that there is a nearly flat band near the Fermi level in optimally doped Bi2212, Bi2201, Y123, and Y124 cuprates.[1–5] The flat band is located near the points $X=\{(\pm\pi,0),(0,\pm\pi)\}$ and has the shape of an elongated saddle aligned with the $X-\Gamma$ line, where $\Gamma=(0,0)$. The flat band in the spectrum leads to a Van Hove singularity in the density of states near the Fermi level. The proximity of the Van Hove singularity to the Fermi level has been used by various theories to account for the high temperature of the superconducting transition.[3,6–8] The existence of the optimal doping level is, naturally, related to the coincidence of the Fermi level with the singularity in the density of states. Note that this common property of all the cuprate superconductors, namely, the existence of a large flat region in the electronic spectrum, is hard to interpret in terms of simple band models.

Important photoemission measurements have been performed in $Sr_2CuO_2Cl_2$,[9] whose CuO_2 planes are in an antiferromagnetic dielectric state. These results yield the hole spectrum in a quantum antiferromagnet and present a good test for numerous theoretical approaches to this problem. The measurements indicated[9] that the band bottom is located near the point $N=(\pi/2,\pi/2)$ and its width is about 0.3 eV. Moreover, the minimum at the bottom is nearly isotropic, i.e., the effective masses in the directions $N-\Gamma$ and $N-X$ are approximately equal.

The features of the quasiparticle spectrum discussed above are often ascribed to strong correlations in the hole motion superposed on a two-dimensional antiferromagnetic background.[10,11] Usually the problem is treated in terms of generalized $t-J$ and Hubbard models, or the three-band model,[12,13] which is more realistic in the case of the CuO_2 plane because it takes into consideration both Cu- and O-orbitals. With due account of the antiferromagnetic background and strong correlations between states at lattice sites, the hole quasiparticle spectrum is dominated, even in the simplest approximation, by the component $\varepsilon(\mathbf{k})\sim(\cos\mathbf{k}_x+\cos\mathbf{k}_y)^2$,[14–17] or, more exactly, the spectrum has a strongly anisotropic minimum at the point N with lines of equal energy elongated along the boundary of the $X-N-X$ magnetic Brillouin zone. The quasiparticles are hole-spin polarons. The latest theoretical studies indicate that it is important to retain a number of real interactions in these models in order to interpret some "fine" features of experimental spectra detected in experiments. These interactions include, for example, the t'-hoppings, which take into account the possibility of hopping to next-nearest-neighbor sites of a square lattice, in the generalized $t-J$ and Hubbard models. In the case of the three-band model, it is important to include in the Hamiltonian direct oxygen-to-oxygen hopping of holes. Note that in the three-band model the t'-interaction effectively takes into account direct oxygen-to-oxygen hopping in the CuO_2 plane. It turned out that with these terms in both models, the strong anisotropy of the spectrum near the bottom is eliminated.[18–22]

This paper considers the effect of some real interactions on the spectrum $\varepsilon(\mathbf{k})$ of the hole-spin polaron in the CuO_2 plane using the three-band Hamiltonian. First of all, the Hamiltonian takes into consideration hopping of an oxygen hole via a copper site with an amplitude τ, including spin-flip processes. The Hamiltonian also takes into account direct O–O hopping of holes with an amplitude h. In addition, we analyze the effect of the hopping trajectory dependence of the amplitude τ on the band spectrum. This dependence does not occur when τ is calculated to lowest order in the $p-d$ hybridization parameter t_{pd} as $\tau=t_{pd}^2/\varepsilon_{pd}$, where $\varepsilon_{pd}=\varepsilon_p-\varepsilon_d$ is the energy difference between the hole levels $Cu(d_{x^2-y^2})$ and $O(p_x,p_y)$. But if terms of higher orders in t_{pd}/ε_{pd} are taken into consideration, the amplitude of the hole hopping τ_{x+y} between the oxygen sites $\mathbf{R}-\mathbf{a}_x$ and $\mathbf{R}+\mathbf{a}_x$ will be different from the amplitude τ_{2x} between the sites $\mathbf{R}-\mathbf{a}_x$ and $\mathbf{R}+\mathbf{a}_x$ (from now on $\mathbf{R}$ is the position of the Cu site, $\pm\mathbf{a}_x$ and $\pm\mathbf{a}_y$ are vectors of oxygen sites closest to

 1063-7761/96/100819-10$10.00

R). A similar dependence of the amplitude on the hopping trajectory results from including $p-d$ hybridization between remote Cu–O orbitals.[23]

We have also studied the effect of temperature and frustration in the spin subsystem on the spectrum $\varepsilon(\mathbf{k})$. It is known that the magnetic correlation length decreases with the doping level. The antiferromagnetic correlation length ξ_{AFM} also falls with the frustration parameter $\alpha=J_2/J_1$, where J_1 and J_2 are the constants of antiferromagnetic exchange between nearest and next nearest neighbors in the square copper sublattice. The similarity between the doping and frustration was demonstrated by Inui *et al.*[24] and confirmed by direct calculations of the spin–spin structural factor $S(\mathbf{q})$ on a 4×4 cluster for the doped $t-J$ model and frustrated Heisenberg model.[25] Naturally, the two models are not completely equivalent. For example, the doped $t-J$ model and frustrated J_1-J_2 model produce different results concerning the dynamic spin-spin structural factor and Raman scattering spectrum.[26] Nonetheless, one may assume that frustration mimics the effect of the finite hole density on static spin correlation functions, from which the spin polaron spectrum is derived. Thus, by calculating the spectrum $\varepsilon(\mathbf{k})$ as a function of frustration, we effectively determine the effect of doping on $\varepsilon(\mathbf{k})$.

The distinguishing feature of our approach is that we treat spin excitations in the spherically symmetrical approximation.[27–29] This approach allows us to investigate a two-dimensional quantum antiferromagnet without invoking the spontaneous symmetry breaking at zero temperature and to describe its paramagnetic state with strong antiferromagnetic correlations, whose ranges are determined by the antiferromagnetic correlation length ξ_{AFM}. This approach seems most adequate for doped HTSC, whose CuO_2 planes have no long-range antiferromagnetic order.

We consider a spin polaron of small radius with spin $S=1/2$ as an elementary hole excitation in our model. The hole excitation operator perturbs the spin subsystem at two copper sites nearest to the hole. The full basis for such a polaron contains ten local operators from which a Bloch combination is constructed. The spectrum is calculated using the projection technique based on delayed two-time Green's functions.

We will demonstrate that by taking into consideration oxygen-oxygen hopping and frustration, we can account for the basic features of the hole excitation spectrum mentioned above and confirmed by experimental data.

In Sec. 2 we will introduce a model Hamiltonian and construct a full basis of local operators to describe the spin polarization at the copper sites closest to an oxygen hole. Then we will derive equations of motion for the Green's functions whose poles determine the spectrum. All the coefficients of the equation system for the Green's functions are listed in Appendix. In Sec. 3 we will present and discuss calculations of the spectrum. Preliminary results of our study were published previously.[30]

2. MODEL HAMILTONIAN AND EQUATIONS OF MOTION FOR THE GREEN'S FUNCTIONS

The effective Hamiltonian for motion of holes in the CuO_2 planes in the three-band model[12,13] has the form[16,31–35]

$$\hat{H}=\hat{T}+\hat{h}+\hat{J}, \tag{1}$$

where

$$\hat{T}=\tau\sum_{\substack{\mathbf{R},\mathbf{a}_1,\mathbf{a}_2,\\ \sigma_1,\sigma_2}} Z_{\mathbf{R}}^{\sigma_1\sigma_2} c^{+}_{\mathbf{R}+\mathbf{a}_2,\sigma_2} c_{\mathbf{R}+\mathbf{a}_1,\sigma_1},$$

$$\hat{h}=-h\sum_{\mathbf{R},\mathbf{a},\mathbf{b},\sigma} c^{+}_{\mathbf{R}+\mathbf{a},\sigma} c_{\mathbf{R}+\mathbf{a}+\mathbf{b},\sigma},$$

$$\hat{J}=\hat{J}_1+\hat{J}_2,\quad \hat{J}_1=\frac{J_1}{2}\sum_{\mathbf{R},\mathbf{g}} \hat{\mathbf{S}}_{\mathbf{R}}\hat{\mathbf{S}}_{\mathbf{R}+\mathbf{g}},$$

$$\hat{J}_2=\frac{J_2}{2}\sum_{\mathbf{R},\mathbf{d}} \hat{\mathbf{S}}_{\mathbf{R}}\hat{\mathbf{S}}_{\mathbf{R}+\mathbf{d}}.$$

The CuO_2 plane is modelled by a square lattice with a constant g and with an elementary cell containing one Cu and two O atoms, $\mathbf{R}$ are positions of copper atoms, $\mathbf{R}+\mathbf{a}$ are positions of four oxygen atoms nearest to the copper: $\mathbf{a}=\pm\mathbf{a}_x$, $\pm\mathbf{a}_y$; $\mathbf{a}_x=g(1/2,0)$, $\mathbf{a}_y=g(0,1/2)$. The following notations are used in Eq. (1): $\mathbf{b}$ are vectors of the nearest neighbors in the oxygen sublattice, $\mathbf{b}=\pm\mathbf{a}_x\pm\mathbf{a}_y$; $\mathbf{g}=2\mathbf{a}$ and $\mathbf{d}=2\mathbf{b}$ are the vectors of the nearest and next nearest neighbors in the copper sublattice. The fermion operator $c^{+}_{\mathbf{R}+\mathbf{a},\sigma}$ and the Hubbard operator $Z_{\mathbf{R}}^{\sigma 0}$ generate a hole with spin $S=1/2$ and spin projection $\sigma/2$ ($\sigma=\pm1$) at oxygen and copper sites, respectively, and the operator $Z_{\mathbf{R}}^{\sigma_1\sigma_2}$ is the Hubbard projection operator which transforms a Cu hole with the spin projection $\sigma_2/2$ to a state with $\sigma_1/2$.

The first term on the right-hand side of Eq. (1) describes a hole hopping from one oxygen site to another via an intermediate copper site with the amplitude $\tau=t_{pd}^2/\varepsilon_{pd}$. The term $\hat{h}$ is responsible for direct O–O hoppings with the amplitude h.

The terms $\hat{J}_1$ and $\hat{J}_2$ correspond to antiferromagnetic interaction between the nearest and next nearest neighbors in the copper sublattice, the frustration parameter is $\alpha=J_2/J_1$. The terms $\hat{T}$ and $\hat{J}_1$ of the effective Hamiltonian in Eq. (1) are derived from the original three-band model using the perturbation theory with respect to t_{pd}/ε_{pd}, where t_{pd} is the parameter of hybridization between the orbitals $O(p)$ and $Cu(d_{x^2-y^2})$; $\varepsilon_{pd}=\varepsilon_d-\varepsilon_p$, ε_p and ε_d are the energies of hole orbitals at the oxygen and copper, respectively. In our model we assume $U_d=\infty$ because the intrasite Coulomb repulsion of two particles generates the largest energy. From estimates of the model parameters on can derive $h\leqslant\tau\sim0.5$ eV and $J\approx0.5\tau$.

As was noted in the Introduction, we relate the term with J_2, which is responsible for frustration in the magnetic Cu subsystem, to the effect of doping.

Let us consider the technique of constructing the basis from local operators $A^{+}_{\mathbf{R},i}$ (i is the operator number) generating one hole in the singlet dielectric state $|G\rangle$ of the CuO_2

plane. It is obvious that all these operator should generate excitations with spin S=1/2 and spin projection $\sigma/2$, This means that the state $A^+_{\mathbf{R},i}|G\rangle$ is an eigenstate of both the operator $\mathbf{S}_{\rm tot}$ of the total spin of copper sites and a hole in the plane, and its projection $S^z_{\rm tot}$:

$$\mathbf{S}_{\rm tot}=\sum_{\mathbf{R}}\left(\mathbf{S}_{\mathbf{R}}+\sum_{\mathbf{a}=\mathbf{a}_x,\mathbf{a}_y}\mathbf{s}_{\mathbf{R}+\mathbf{a}}\right). \tag{2}$$

Here $\mathbf{s}_{\mathbf{R}+\mathbf{a}}$ is the oxygen-hole spin operator.

The first two operators, $A^+_{\mathbf{R},1(2)}$, obviously generate holes at two oxygen sites of an elementary cell without perturbing the copper spin subsystem:

$$A^+_{\mathbf{R},1}=c^+_{\mathbf{R}+\mathbf{a}_x,\sigma},\quad A^+_{\mathbf{R},2}=c^+_{\mathbf{R}+\mathbf{a}_y,\sigma}. \tag{3}$$

The operator basis can be enhanced in a natural way by taking commutators of the operators $A_{\mathbf{R},1(2)}$ with the hopping Hamiltonian $\hat{T}$. One can check that the result is four new operators, $A^+_{\mathbf{R},3(4)}$ and $A^+_{\mathbf{R},5(6)}$, generating hole excitations in the state $|G\rangle$ of the CuO_2 plane:

$$A^+_{\mathbf{R},3(4)}=\sigma\sum_{\gamma=\pm\sigma}\gamma Z^{\bar{\gamma}\bar{\sigma}}_{\mathbf{R}}c^+_{\mathbf{R}+\mathbf{a}_x(\mathbf{a}_y),\gamma},$$

$$A^+_{\mathbf{R},5(6)}=\sigma\sum_{\gamma=\pm\sigma}\gamma Z^{\bar{\gamma}\bar{\sigma}}_{\mathbf{R}+\mathbf{g}_x(\mathbf{g}_y)}c^+_{\mathbf{R}+\mathbf{a}_x(\mathbf{a}_y),\gamma}. \tag{4}$$

Hereafter we assume that $\bar{\sigma}=-\sigma$.

The operators defined by Eq. (4) generate holes at oxygen sites concurrently with a spin excitation at a neighboring copper site. Note that if the operators in Eq. (4) act on a state of a two-site Cu–O system containing one hole at the copper site $\mathbf{R}$ with $S=1/2$ and $S^z=\bar{\sigma}/2$, the resulting two-hole state is singlet. It is obvious that in this sense the linear combination of the operators in Eq. (4), i.e.,

$$A^+_{\mathbf{R},3}+A^+_{\mathbf{R},4}+A^+_{\mathbf{R}-g_x,5}\,A^+_{\mathbf{R}-g_y,6},$$

is similar to the Zhang–Rice spin polaron.[39]

The next step in the enhancement of the basis is calculating commutators of the terms $\hat{T}$ and $\hat{J}$ in the Hamiltonian defined by Eq. (1) with excitation operators given by Eq. (4). We select from the resulting operators only those which are, firstly, linearly independent of those defined by Eqs. (3) and (4), secondly, generate excitations at two sites of the copper sublattice nearest to the oxygen site with the hole. As a result, we have four new operators $A^+_{\mathbf{R},i}$ where $i=7-10$:

$$A^+_{\mathbf{R},7(8)}=\sigma\sum_{\gamma,\lambda=\pm\sigma}\gamma(Z^{\bar{\gamma}\lambda}_{\mathbf{R}}Z^{\lambda\bar{\sigma}}_{\mathbf{R}+\mathbf{g}_x(\mathbf{g}_y)}-Z^{\bar{\gamma}\lambda}_{\mathbf{R}+\mathbf{g}_x(\mathbf{g}_y)}Z^{\lambda\bar{\sigma}}_{\mathbf{R}})c^+_{\mathbf{R}+\mathbf{a}_x(\mathbf{a}_y),\gamma},$$

$$A^+_{\mathbf{R},9(10)}=\mathbf{S}_{\mathbf{R}}\mathbf{S}_{\mathbf{R}+\mathbf{g}_x(\mathbf{g}_y)}c^+_{\mathbf{R}+\mathbf{a}_x(\mathbf{a}_y),\sigma}. \tag{5}$$

Similar operators of a spin polaron which occupies three sites were discussed by Emery[12] and Ding *et al.*[40]

The operators $A_{\mathbf{R},i}$, $(i=5-10)$, by definition describe excitations with $S_{\rm tot}=1/2$ and $S^z_{\rm tot}=\sigma/2$ since the operator $\mathbf{S}_{\rm tot}$ and its projection $S^z_{\rm tot}$ commute with each of the terms in the Hamiltonian. One can prove that the operators $A_{\mathbf{R},i}$, $(i=1-10)$, form a full basis of local operators for a short-range spin polaron (only copper spins closest to the oxygen hole are excited) with $S_{\rm tot}=1/2$.

In order to determine the spin polaron spectrum $\varepsilon(\mathbf{k})$, we use retarded two-time Green's functions $G_{ij}(t,\mathbf{k})$ defined in terms of the Fourier transforms $A_{\mathbf{k},i}$ of the previously described ten operators $A_{\mathbf{R},i}$:

$$G_{ij}(t,\mathbf{k})\equiv\langle A_{\mathbf{k},i}(t)|A^+_{\mathbf{k},j}(0)\rangle=-i\theta(t)\times\langle[A_{\mathbf{k},i}(t),A^+_{\mathbf{k},j}(0)]\rangle,$$

$$A_{\mathbf{k},j}=\frac{1}{\sqrt{N}}\sum_{\mathbf{R}}e^{i\mathbf{k}\mathbf{R}}A_{\mathbf{R},j},\quad i,j=1-10. \tag{6}$$

The equations of motion for Fourier transforms of the Green's functions have the form

$$\omega\langle A_{\mathbf{k},i}|A^+_{\mathbf{k},j}\rangle_\omega=K_{i,j}+\langle B_{\mathbf{k},i}|A^+_{\mathbf{k},j}\rangle_\omega,$$

$$K_{i,j}=\langle[A_{\mathbf{k},i},A^+_{\mathbf{k},j}]\rangle,\quad B_{\mathbf{k},i}=[A_{\mathbf{k},i},H]. \tag{7}$$

In the standard Mori–Zwanzig projection technique[41] we approximate the new operators $B_{\mathbf{k},i}$ by their projections on the space $\{A_{\mathbf{k},i}\}$ of basis operators:

$$B_{\mathbf{k},i}\simeq\sum_l\Omega_{i,l}(\mathbf{k})A_{\mathbf{k},l},\quad\Omega(\mathbf{k})=D(\mathbf{k})K^{-1},$$

$$D_{ij}(\mathbf{k})=\langle[B_{\mathbf{k},i},A^+_{\mathbf{k},l}]\rangle. \tag{8}$$

After we substitute the approximate expressions for the operators $B_{\mathbf{k},i}$ in Eq. (8) into the equations of motion (7), the equation system (7) for Green's functions $\langle A_{\mathbf{k},i}|A^+_{\mathbf{k},j}\rangle_\omega$ becomes closed and can be presented in the matrix form

$$(\omega E-DK^{-1})G=K, \tag{9}$$

where E is the unit matrix.

The quasiparticle spectrum $\varepsilon(\mathbf{k})$ is determined by the poles of the Green's function G and can be derived from the condition $\det|K\varepsilon(\mathbf{k})-D|=0$. Note that this procedure is equivalent to the variational procedure of constructing a wave function of a short-range polaron.[18] The calculation of elements of the arrays D and K is not difficult but is lengthy because it involves calculation of commutators of complex operators $A_{\mathbf{k},i}$ and $B_{\mathbf{k},i}$. The elements are expressed in terms of two-site and three-site correlators of Hubbard operators for copper states. The copper states are described by the frustrated Heisenberg model with the Hamiltonian $\hat{J}$.

From the spherical symmetry of the copper spin subsystem, the three-site correlators can be reduced to two-site correlators. Typical relations between these correlators are given in the Appendix. The elements of the arrays D and K in the explicit form are also given there.

Thus, the spectrum calculation demands spin pair-correlation functions $C_r=\langle\mathbf{S}_{\mathbf{R}}\mathbf{S}_{\mathbf{R}+\mathbf{r}}\rangle$ expressed as functions of the separation between the sites, temperature, and frustration. These functions were derived in our previous work[27] using the spherically symmetrical theory of spin waves and have been used in this study.

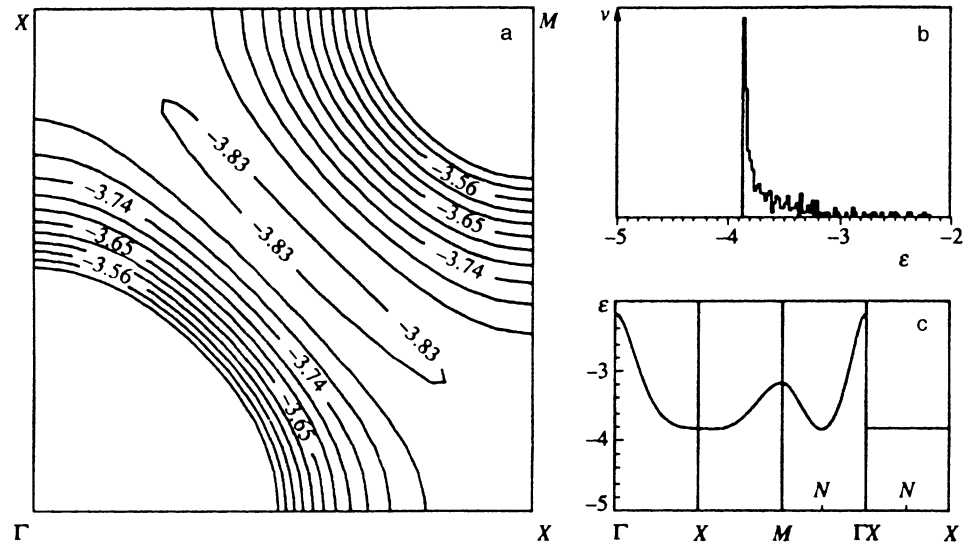

FIG. 1. Spectrum $\varepsilon(\mathbf{k})$ at $T=0$, $\alpha=J_1/J_2=0.4$, $h=0$: (a) contours of constant energy in the first quadrant of the Brillouin zone; (b) density of states $\nu(\varepsilon)$; (c) energy spectrum along symmetrical directions.

3. RESULTS AND DISCUSSION

In this section we give only calculations of the function $\varepsilon(\mathbf{k})$ in the lowest band, i.e., the lowest eigenvalues of the operator DK^{-1} at fixed $\mathbf{k}$. This band determines the conducting properties at low doping levels.

Note an important feature of our technique, which should be taken into account when comparing our results to calculations by other authors.

In order to make the signs of hopping integrals in $\hat{T}$ and $\hat{h}$ in Eq. (1) to be independent of the hopping direction, we had to perform a unitary transformation changing the phases of the $\mathrm{Cu}(d_{x^2-y^2})$ and $\mathrm{O}(p)$ wave functions.[42-44] This was done by multiplying local wave functions by the factor $\exp(i\mathbf{Q}\cdot\mathbf{R})$, where $\mathbf{R}$ is the radius-vector of the corresponding elementary cell and $\mathbf{Q}=(\pi/g,\pi/g)$ is the antiferromagnetic vector (below the copper sublattice constant is taken $g=1$). In order to restore the initial translational symmetry of local wave functions, we replace $\varepsilon(\mathbf{k})$ by $\varepsilon(\mathbf{k}+\mathbf{Q})$ and present our results in these variables.

In all the plots except Fig. 6, the calculated spectra correspond to the typical value of the exchange integral $J_1=0.2\tau$ at two values of the frustration parameter, $\alpha=0$ and 0.4, and two values of the oxygen–oxygen hopping integral, $h=0$ and 0.4τ. We recall that the energy parameters τ and J_1 and the parameters of the initial model t_{pd} and ε_{pd} are related to each other:[16,31-35]

$$\tau=\frac{t_{pd}^2}{\varepsilon_{pd}},\quad J_1=\frac{4\tau^2}{\varepsilon_{pd}}. \tag{10}$$

The calculated spectra are shown by contours of constant energy drawn with equal energy increments in the first quadrant of the first Brillouin zone. The energies of some of the contours are given in the graphs. The densities of states $\nu(\varepsilon)$ and curves of $\varepsilon(\mathbf{k})$ along symmetrical directions $\Gamma-X-M-\Gamma$ and $X-N-X$ $[M=(\pi,\pi),\ N=(\pi/2,\pi/2)]$ are also plotted in the graphs. The unit energy is τ.

As was noted in the Introduction, the calculated spectra $\varepsilon(\mathbf{k})$ are interpreted assuming that an increase in the frustration parameter α simulated higher doping level.

Figure 1 shows the spectrum $\varepsilon(\mathbf{k})$ at $h=0$, $T=0$, and the finite frustration parameter $\alpha=0.4$. The spectrum has a minimum near the point N. In a wide region about the boundary of the antiferromagnetic Brillouin zone $X-N-X$ there is a flat band in which the energy is a weak function of $\mathbf{k}$ (Fig. 1c). This portion of the spectrum near the bottom generates a peak in the density of states (Fig. 1b) whose shape is similar to that of a one-dimensional singularity: $\nu(\varepsilon)\propto\varepsilon^{-1/2}$.

At the minimum, the spectrum is highly anisotropic, as can be seen in Fig. 1c, i.e., the effective masses around the point N in the directions $N-M$ and $N-X$ are very different. At a low filling, the Fermi surface is an ellipse and the Hall constant R_H should have the "hole" sign, $R_H>0$.

We do not show the shape of $\varepsilon(\mathbf{k})$ for $T=0$, $h=0$, and $\alpha=0$. In this case the spectrum has a flat portion around the line $X-N-X$, but the weak modulation of the spectrum near the band bottom is slightly different, so the minimum is on the line $X-\Gamma$ near the point X.

The spectrum is radically different at zero frustration factor ($\alpha=0$), but with oxygen–oxygen hopping. One can see in Figs. 2a and 2c that at $h=0.4$ the minimum of the band bottom is still near the point N. But unlike the case shown in Fig. 1 ($h=0$), this minimum is isotropic. As was noted in the Introduction, this shape of the minimum is observed at zero doping[9] (in our case this corresponds to zero frustration). One may assume that the isotropic minimum near the band bottom is due to oxygen–oxygen hopping. The authors of Refs. 19 and 20 came to similar conclusions.

Another feature of the spectrum in Fig. 2a and 2c for $h\neq 0$ seen by comparing it with Fig. 1a and 1c is a notable modulation around the minimum and a flat portion near the point X. As a result, there is a second peak in the density of states (Fig. 2b). It is interesting that the band portion responsible for the second peak has the shape of an elongated saddle. But this saddle is aligned with the direction $X-M$,

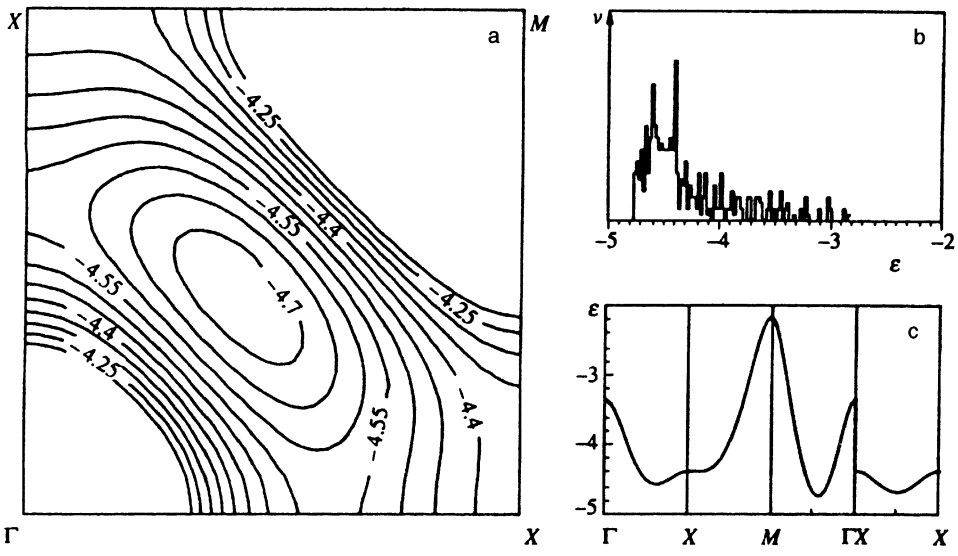

FIG. 2. Same as Fig. 1, for $T=0$, $\alpha=J_2/J_1$ and $h=0.4$.

as can be seen in Fig. 2a, whereas the experimentally detected feature is extended along the direction $X-\Gamma$.[1-5]

Now let us consider the case of zero temperature, but with both frustration factor and oxygen–oxygen hopping amplitude nonzero ($\alpha=0.4$, $h=0.4$), shown in Fig. 3. In this case the spectrum $\varepsilon(\mathbf{k})$ is radically different from that in Fig. 2, since its elongated saddle point is aligned with the line $X-\Gamma$, which is in agreement with experiments performed at an optimal doping level (i.e., in our language, at a finite frustration). One can check that at a higher frustration (doping) parameter, this feature and the resulting peak in the density of states are less pronounced. This result is consistent with the general concept that the transition temperature drops in overdoped HTSC if we assume that high-T_c superconductivity is caused by the proximity of the Fermi level to the Van Hove singularity of the higher peak on the $\nu(\varepsilon)$ curve in Fig. 3b.

If the Fermi level coincides with an equal-energy curve near the elongated saddle, for example, the line with $\varepsilon=-4.43$ in Fig. 3a, the Fermi surface should have a second portion around the point M. Note that the Hall constant is directly related to a weighted integral of the curvatures of these lines.[45] One can easily check that the two contours have curvatures of different signs, so the Hall constant may change its sign from plus to minus as the doping level increases.

Note that the comparison of spectra shown in Figs. 2a and 2c ($h=0.4$, $\alpha=0$) and 3a and 3c ($h=0.4$, $\alpha=0.4$) demonstrates that the spectrum of the CuO_2 plane cannot be described at all in the rigid-band approximation.

Our calculations at finite temperatures indicate that, like the frustration, the temperature effectively changes the spectrum. For example, the spectrum calculated for $h=0.4$, $\alpha=0$, and $T=J_1$ fits to the curves in Fig. 3 for $h=0.4$, $\alpha=0.4$, and $T=0$ well. This is not surprising because the spectrum is controlled by correlation functions. In our previous publication[27] we proved that at moderate frustration parameters $\alpha<0.5$ an increase in both T and α leads to lower

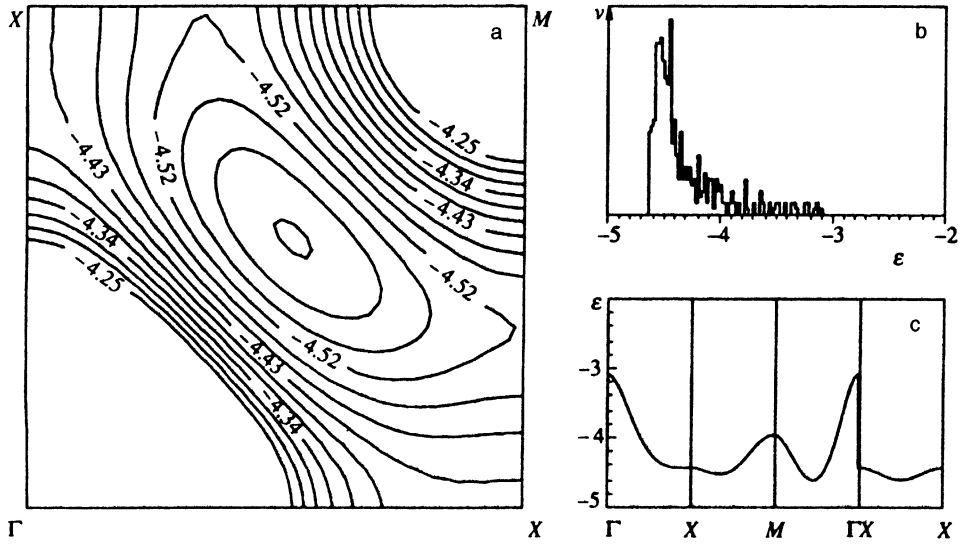

FIG. 3. Same as Fig. 1 at $T=0$, $\alpha=J_2/J_1$, and $h=0.4$.

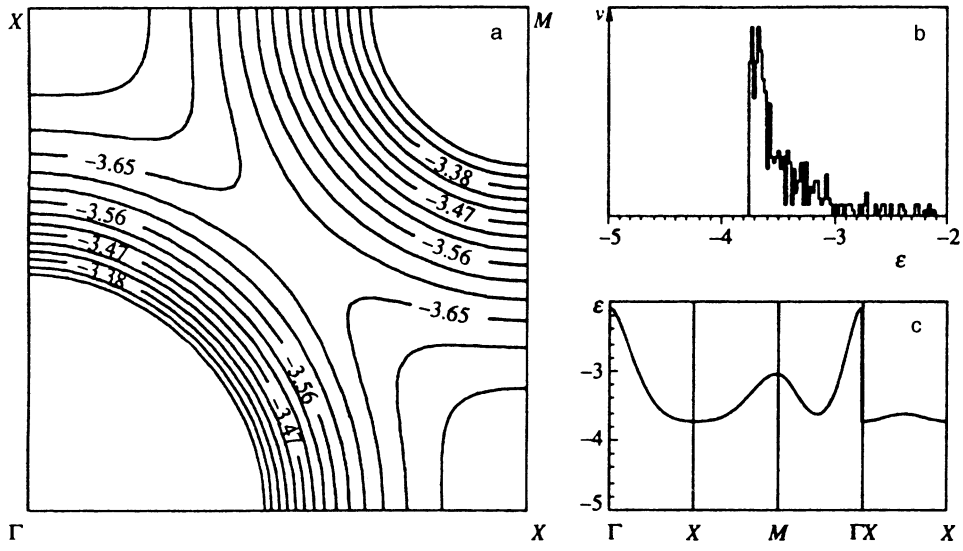

FIG. 4. Same as Fig. 1, but with the anisotropy of the hopping amplitude $\Delta\tau/\tau=-0.15$.

antiferromagnetic correlations (although it is hard to correctly translate one effect into another).

Now let us turn to the effect of the hopping amplitude on the spectrum. The modified component $\hat{T}$ of the Hamiltonian defined by Eq. (1) takes the form

$$\hat{T}=\sum_{\substack{\mathbf{R},\mathbf{a}_1,\mathbf{a}_2,\\ \sigma_1,\sigma_2}}(\tau+\Delta\tau\delta_{\mathbf{a}_2,-\mathbf{a}_1})Z_{\mathbf{R}}^{\sigma_1\sigma_2}c^{+}_{\mathbf{R}+\mathbf{a}_2,\sigma_2}c_{\mathbf{R}+\mathbf{a}_1,\sigma_1}. \tag{11}$$

The Hamiltonian in Eq. (11) takes into account that the hole hopping described by the vectors $\pm\mathbf{a}_x$ and $\pm\mathbf{a}_y$ has the amplitude τ, and that described by the vectors $\pm2\mathbf{a}_x$ and $\pm2\mathbf{a}_y$ has an amplitude $\tau+\Delta\tau$. The physical cause of the difference between these amplitudes was discussed in the Introduction. Figures 4 and 5 show spectra calculated for $T=0$, $h=0$, $\alpha=0.4$, and $\Delta\tau/\tau=-0.15$ and 0.15, respectively. One can see in Fig. 4 that the spectrum calculated for $\Delta\tau<0$ is radically different from all other spectra. The most remarkable feature is that the local minimum at the point N disappears. But this situation, apparently, is not realized because calculations by the singlet-triplet model yield an estimate $\Delta\tau\sim0.1\tau>0$. The comparison of spectra in Fig. 5 ($T=0$, $\alpha=0.4$, $h=0$, and $\Delta\tau/\tau=0.15$) and Fig. 3 ($T=0$, $\alpha=0.4$, $h=0.4$ and $\Delta\tau/\tau=0$) with that shown in Fig. 1 ($T=0$, $\alpha=0.4$, $h=0$, and $\Delta\tau/\tau=0$) demonstrates that the inclusion of $\Delta\tau>0$ is equivalent to a higher amplitude of oxygen–oxygen hopping.

There are few calculations by the three-band model which yield fairly complete information about the spectrum. Dopf *et al.*[46,47] calculated the three-band spectrum by the quantum Monte Carlo technique, and Putz *et al.*[48] by finding a self-consistent solution of the Dyson equation to the one-particle Green's function with due account of the interaction between a hole and fluctuations of charge and spin densities. These calculations were based on the three-band model with typical values of parameters: $\varepsilon_{pd}=4t_{pd}$, $U_d=6t_{pd}$, the tem-

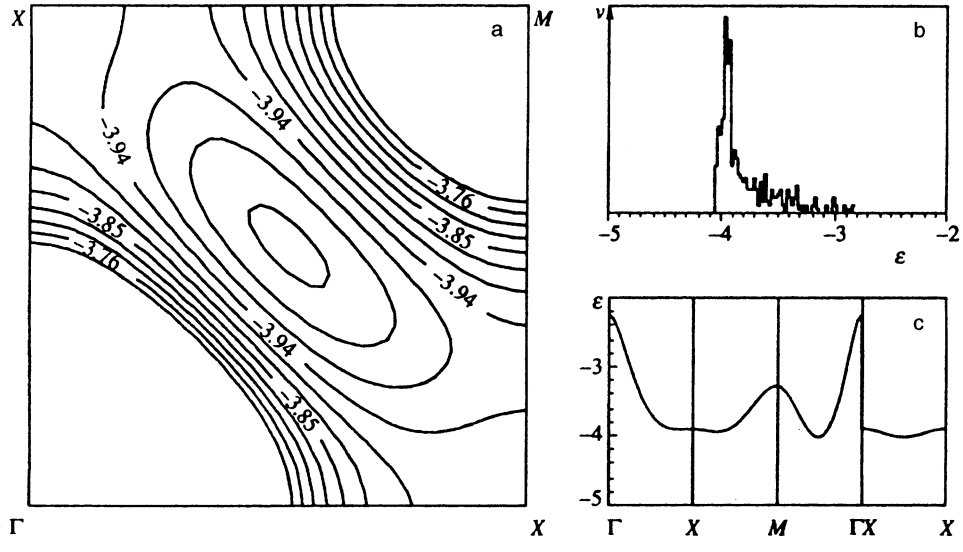

FIG. 5. Same as Fig. 1, but with the anisotropy of the hopping amplitude $\Delta\tau/\tau=0.15$.

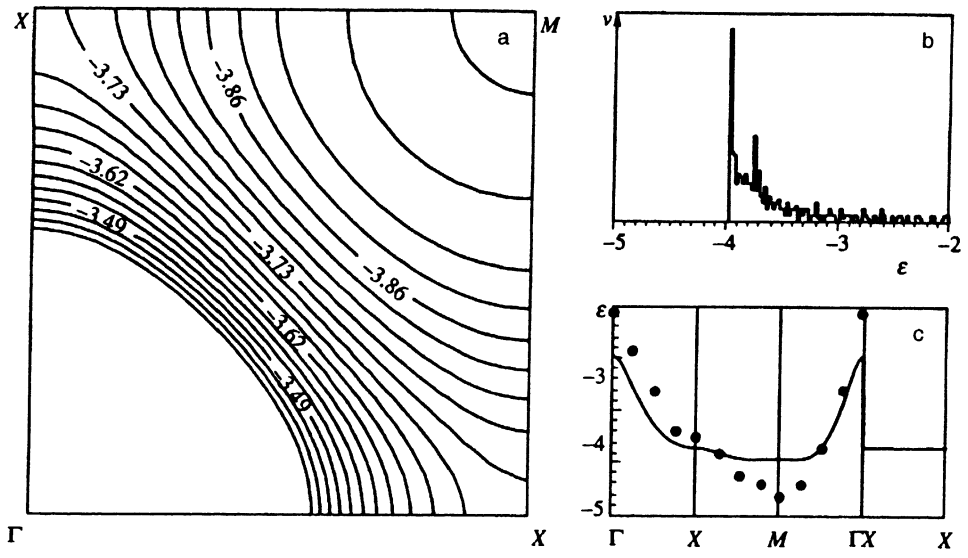

FIG. 6. (a) Contours of constant energy of the spectrum $\varepsilon(\mathbf{k})$ for $J_1=0.25$, $T=1.6J_1$, $\alpha=J_2/J_1=0.4$, and $h=0.4$; (b) density of states $\nu(\varepsilon)$; (c) spectrum $\varepsilon(\mathbf{k})$ plotted along symmetrical directions: solid trace shows results of the present work (at the same parameters as in Fig. 6a); dots show Monte Carlo calculations by the three-band model[46,47] for $\varepsilon_{pd}=4t_{pd}$, $U_d=6t_{pd}$, $T=0.1t_{pd}$, and $\delta=0.25$. The energy unit is τ, and $t_{pd}=4\tau$. The energy axis for the Monte Carlo calculations is shifted arbitrarily.

perature $T=0.1t_{pd}$, and the doping level $\delta=0.25$. Our results are compared to those of Ref. 48 in Fig. 6, which shows the spectrum $\varepsilon(\mathbf{k})$ at similar parameters of our effective Hamiltonian, namely $J_1=0.25\tau$, $T=1.6J_1$, $\alpha=0.4$, and $h=0.4\tau$. The selection of the latter parameters was based on Eq. (10) with $t_{pd}/\varepsilon_{pd}=0.25$. Note that Eq. (10) is valid only for $U_d=\infty$, i.e., this comparison is intended to show the general trend. Figure 6 demonstrates that the band bottom is at the point M because the high temperature breaks antiferromagnetic correlations. Nonetheless, the saddle point near X persists. Figure 6c also shows a Monte Carlo calculation of the spectrum, which is quite similar to that in Ref. 48, and our calculations along symmetrical directions. One can see that at high temperature the results are fairly close, although the parameter U_d is different, and the doping $\delta=0.25$ is simulated by the frustration $\alpha=0.4$.

Let us also mention calculations[49–51] based on the "cluster perturbation" theory, which reduces the three-band model to a generalized $t-J$ model taking into account t' hoppings to second and t'' to third nearest neighbors. As was noted in Introduction, the inclusion of the t' hopping, which efficiently simulate direct oxygen-oxygen hoppings in the initial model, makes the band near its bottom at the point N isotropic,[19] which is in agreement with our results. This effect also occurs when t'' hoppings are taken into account.[51] In the recent work[51] the parameters of the Hamiltonian describing the t, t', and t'' hoppings were derived from realistic parameters of the three-band model. Unfortunately, the frustration was not included in these calculations, the model was based on two magnetic sublattices, and the approximation used yielded a spectrum periodic in agreement with the shape of the magnetic Brillouin zone. This means that no extended Van Hove singularity on the $X-\Gamma$ line could be obtained without a similar singularity on the $X-M$ line. It is difficult, therefore, to compare our results to those reported in Ref. 51.

In conclusion, let us spell out the basic result of our analysis of the model. There are several important mechanisms, not mutually exclusive, generating singularities in the CuO_2-plane hole spectrum similar to those detected in experiments. The band bottom may become isotropic because of either oxygen-oxygen hopping with amplitude h or the dependence of the hopping amplitude τ on the trajectory. The saddle-like singularity aligned with the $X-\Gamma$ line is generated when, firstly, the frustration (doping) and oxygen–oxygen hopping are taken into account concurrently, secondly, when account is taken of the finite temperature and frustration, and thirdly, when frustration occurs and the hopping amplitude depends on the trajectory. The basic result of our study is the conclusion that with due account of realistic features of the model, one can interpret experimentally observed spectra of hole excitations.

In our opinion, additional interactions, such as Coulomb repulsion of holes at neighboring copper and oxygen sites, and modifications of the effective Hamiltonian in Eq. (1), which applies, strictly speaking, only for $t_{pd}\ll\varepsilon_{pd}$, should not radically change our results. But this issue, as well as calculations taking account of interaction between holes (polarons in our case), deserves further investigation, especially in the hole concentration range corresponding to optimal doping.

The work was supported by the International Association for Cooperation with Scientists of the former Soviet Union (Grant INTAS-93-285), the Russian Fund for Fundamental Research (Grant No. 95-02-04239a), the Russian National Program on Superconductivity (Grant No. 93080), and the International Soros Program of Education in the Exact Sciences (Grant a883-f).

APPENDIX

Here we give some formulas for spin correlation functions that are used in the calculations of the matrix elements D_{ij} and K_{ij} in Eq. (8) and the explicit expressions for these elements.

Commutators of the operators $B_{\mathbf{k},i}$ and $A_{\mathbf{k},i}$ yield statistical averages over states of the spin subsystem of products

of two and three Hubbard operators located at different copper sites. If the spherical symmetry of the spin subsystem is used, the three-site averages can be reduced to two-site averages, and they in turn are reduced to scalar products of spin operators. Correlation functions of spin operators with due account of temperature and frustration were calculated previously[27] in the spherically symmetrical theory of spin waves. Below some typical relations for local correlation functions and some operator relations are listed:

$$\sum_{\sigma} Z_{\mathbf{R}}^{\sigma\sigma}=1, \quad Z_{\mathbf{R}}^{\sigma\sigma}=\frac{1}{2}+\sigma S_{\mathbf{R}}^{z},$$

$$\sum_{\sigma,\gamma=\pm\sigma} Z_{\mathbf{R}_1}^{\sigma\gamma}Z_{\mathbf{R}_2}^{\gamma\sigma}=\frac{1}{2}+2\mathbf{S}_{\mathbf{R}_1}\mathbf{S}_{\mathbf{R}_2},$$

$$Z_{\mathbf{R}_1}^{\sigma\sigma}Z_{\mathbf{R}_2}^{\sigma\sigma}=\frac{1}{4}+\frac{\sigma}{2}\,(S_{\mathbf{R}_1}^{z}+S_{\mathbf{R}_2}^{z})+S_{\mathbf{R}_1}^{z}S_{\mathbf{R}_2}^{z},$$

$$\sum_{\gamma=\pm\sigma} Z_{\mathbf{R}_1}^{\sigma\gamma}Z_{\mathbf{R}_2}^{\gamma\sigma}=\frac{1}{4}+\frac{\sigma}{2}\,(S_{\mathbf{R}_1}^{z}+S_{\mathbf{R}_2}^{z})+\mathbf{S}_{\mathbf{R}_1}\mathbf{S}_{\mathbf{R}_2} -i\sigma(S_{\mathbf{R}_1}^{x}S_{\mathbf{R}_2}^{y}-S_{\mathbf{R}_1}^{y}S_{\mathbf{R}_2}^{x}),$$

$$\sum_{\gamma=\pm\sigma} \langle Z_{\mathbf{R}_1}^{\sigma\gamma}Z_{\mathbf{R}_2}^{\gamma\sigma}\rangle=\frac{1}{4}+C_{R_{12}},$$

$$\sum_{\lambda=\pm\sigma} \langle Z_{\mathbf{R}_1}^{\sigma\lambda}Z_{\mathbf{R}_2}^{\lambda\sigma}Z_{\mathbf{R}_3}^{\gamma\gamma}\rangle=\frac{1}{8}+\frac{1}{2}\,C_{R_{12}} +\frac{1}{6}\,\sigma\gamma(C_{R_{23}}+C_{R_{31}}),$$

$$\sum_{\gamma=\pm\sigma} \langle Z_{\mathbf{R}_1}^{\bar{\sigma}\gamma}Z_{\mathbf{R}_2}^{\gamma\sigma}Z_{\mathbf{R}_3}^{\sigma\bar{\sigma}}\rangle=\frac{1}{3}\,(C_{R_{23}}+C_{R_{31}}),$$

$$\sum_{\lambda,\gamma=\pm\sigma} \langle Z_{\mathbf{R}_1}^{\sigma\gamma}Z_{\mathbf{R}_2}^{\gamma\lambda}Z_{\mathbf{R}_3}^{\lambda\sigma}\rangle=\frac{1}{8}+\frac{1}{2}\,(C_{R_{12}}+C_{R_{23}}+C_{R_{31}}). \tag{A1}$$

In Eqs. (A1) all the sites in one formula are different, and we use the notations $C_{R_{12}}=\langle \mathbf{S}_{\mathbf{R}_1}\mathbf{S}_{\mathbf{R}_2}\rangle$ and $R_{12}=|\mathbf{R}_1-\mathbf{R}_2|$.

It is more convenient to calculate the elements of the arrays D and K in Eq. (8) in the new basis of the operators $\tilde{A}_{\mathbf{R},i}^{+}$, which can be expressed as linear combinations of the operators of the initial basis:

$$\tilde{A}_{\mathbf{R},i}^{+}=A_{\mathbf{R},i}^{+}, \quad i=1-6,$$

$$\tilde{A}_{\mathbf{R},7(8)}^{+}=\frac{1}{2}\left(-A_{\mathbf{R},7(8)}^{+}-2A_{\mathbf{R},9(10)}^{+}+A_{\mathbf{R},1(2)}^{+}-A_{\mathbf{R},5(6)}^{+} +\frac{1}{2}\,A_{\mathbf{R},3(4)}^{+}\right),$$

$$\tilde{A}_{\mathbf{R},9(10)}^{+}=\frac{1}{2}\left(-A_{\mathbf{R},7(8)}^{+}+2A_{\mathbf{R},9(10)}^{+}+A_{\mathbf{R},1(2)}^{+}-A_{\mathbf{R},5(6)}^{+} -\frac{1}{2}\,A_{\mathbf{R},3(4)}^{+}\right). \tag{A2}$$

The new operators are transformed to one another under reflection with respect to the oxygen site, i.e., if the site indices in the Hubbard operators located at copper sites in $\tilde{A}_{\mathbf{R},i}^{+}$ are transformed according to $\mathbf{R}\to\mathbf{R}+\mathbf{g}_x(\mathbf{g}_y)$, $\mathbf{R}+\mathbf{g}_x(\mathbf{g}_y)\to\mathbf{R}$, the following relations hold:

$$\tilde{A}_{\mathbf{R},1(2)}^{+}(\mathbf{R}\leftrightarrow\mathbf{R}+\mathbf{g}_x(\mathbf{g}_y))=\tilde{A}_{\mathbf{R},1(2)}^{+},$$

$$\tilde{A}_{\mathbf{R},3(4)}^{+}(\mathbf{R}\leftrightarrow\mathbf{R}+\mathbf{g}_x(\mathbf{g}_y))=\tilde{A}_{\mathbf{R},5(6)}^{+},$$

$$\tilde{A}_{\mathbf{R},7(8)}^{+}(\mathbf{R}\leftrightarrow\mathbf{R}+\mathbf{g}_x(\mathbf{g}_y))=-\tilde{A}_{\mathbf{R},9(10)}^{+}. \tag{A3}$$

Here the transformation is denoted as $\mathbf{R}\leftrightarrow\mathbf{R}+\mathbf{g}_x(\mathbf{g}_y)$.

Given the relations (A3), it is sufficient to calculate the following elements:

$$D_{11}(\mathbf{k})=\tau+\tau_1\cos k_x,$$

$$D_{21}(\mathbf{k})=2(\tau-2h)\cos\frac{k_x}{2}\cos\frac{k_y}{2},$$

$$D_{31}(\mathbf{k})=\tau_1\left[L_2u^2-\frac{1}{2}\,(u^*)^2\right]-\tau L_1,$$

$$D_{41}(\mathbf{k})=\tau\cos\frac{k_x}{2}\,(2L_2v-v^*)-2h\cos\frac{k_x}{2}\cos\frac{k_y}{2},$$

$$D_{71}(\mathbf{k})=\tau_1[2(u^*)^2-u^2]L_2+\tau L_2,$$

$$D_{81}(\mathbf{k})=2\tau L_2\cos\frac{k_x}{2}\,(2v^*-v)-4hL_2\cos\frac{k_x}{2}\cos\frac{k_y}{2},$$

$$D_{33}(\mathbf{k})=-\frac{\tau}{2}-2\tau_1L_1\cos k_x-4J_1(C_g+\alpha C_d),$$

$$D_{43}(\mathbf{k})=-(\tau+h)(uv^*+L_1(uv+u^*v^*)-L_3vu^*) -h(3L_3+2C_g)vu^*,$$

$$D_{53}(\mathbf{k})=\tau_1[-u^2+L_4(u^*)^2]-2\tau L_1+J_1C_g,$$

$$D_{73}(\mathbf{k})=L_2[\tau_1(u^*-2u)+2\tau]-J_1[3L_3 +(C_{2g}-C_d)/2-\alpha L_5],$$

$$D_{83}(\mathbf{k})=\tau L_2(uv^*+u^*v^*-2uv)-\frac{\tau}{2}\left(\frac{1}{4}-C_d\right)vu^* -h\left[L_2(2uv-uv^*)+L_3u^*v^* +\frac{1}{2}\left(\frac{1}{4}-C_d\right)vu^*\right],$$

$$D_{93}(\mathbf{k})=\tau_1\left[\left(\frac{1}{4}-C_{2g}\right)\frac{(u^*)^2}{2}-L_2u^2\right]+\tau L_2-J_1(3L_3 +C_{2g}-C_d/2-\alpha L_5),$$

$$D_{77}(\mathbf{k})=2\tau_1L_4\cos k_x-2\tau L_2+J_1\left(\frac{3}{4}-9C_g+4C_d +2C_{2g}-4\alpha L_5\right),$$

$$D_{87}(\mathbf{k})=\tau L_3(uv-2vu^*+u^*v^*+uv^*)-2hL_3\Big[uv^*+vu^*-\frac{1}{2}(uv+u^*v^*)\Big],$$

$$D_{97}(\mathbf{k})=\tau_1 L_4[2(u^*)^2-u^2]-4\tau L_2+J_1\Big(\frac{3}{4}-6C_g+2C_d+C_{2g}-2\alpha L_5\Big).$$

Here we use the notations $u=\exp(ik_x/2)$ and $v=\exp(ik_y/2)$; an asterisk denotes complex conjugation.

In the correlation functions $C_r=\langle \mathbf{S}_i\mathbf{S}_{i+r}\rangle$ and their indices, we use the following notations: $g=|\mathbf{g}_x|=|\mathbf{g}_y|$, $d=|\pm\mathbf{g}_x\pm\mathbf{g}_y|$, $f=|\pm 2\mathbf{g}_x\pm\mathbf{g}_y|=|\pm 2\mathbf{g}_y\pm\mathbf{g}_x|$, $L_1=1/4+C_g$, $L_2=1/4-C_g$, $L_3=1/8-C_g+C_d/2$, $L_4=1/8-C_g+C_{2g}/2$, $L_5=2C_d-C_g-C_f$.

The rest of the elements are expressed in terms of those listed above:

$$D_{51}(k_x,k_y)=D_{31}(-k_x,k_y);\quad D_{61}(k_x,k_y)=D_{41}(k_x,-k_y);$$

$$D_{91}(k_x,k_y)=-D_{71}(-k_x,k_y);\quad D_{10,1}(k_x,k_y)=-D_{81}(k_x,-k_y);$$

$$D_{22}(k_x,k_y)=D_{11}(k_y,k_x);\quad D_{32}(k_x,k_y)=D_{41}(k_y,k_x);$$

$$D_{42}(k_x,k_y)=D_{31}(k_y,k_x);\quad D_{52}(k_x,k_y)=D_{61}(k_y,k_x);$$

$$D_{62}(k_x,k_y)=D_{51}(k_y,k_x);\quad D_{72}(k_x,k_y)=D_{81}(k_y,k_x);$$

$$D_{82}(k_x,k_y)=D_{71}(k_y,k_x);\quad D_{92}(k_x,k_y)=D_{10,1}(k_y,k_x);$$

$$D_{10,2}(k_x,k_y)=D_{91}(k_y,k_x);\quad D_{63}(k_x,k_y)=D_{43}(k_x,-k_y);$$

$$D_{10,3}(k_x,k_y)=-D_{83}(k_x,-k_y);\quad D_{44}(k_x,k_y)=D_{33}(k_y,k_x);$$

$$D_{54}(k_x,k_y)=D_{43}(k_y,-k_x);\quad D_{64}(k_x,k_y)=D_{53}(k_y,k_x);$$

$$D_{74}(k_x,k_y)=D_{83}(k_y,k_x);\quad D_{84}(k_x,k_y)=D_{73}(k_y,k_x);$$

$$D_{94}(k_x,k_y)=-D_{83}(k_y,-k_x);\quad D_{10,4}(k_x,k_y)=D_{93}(k_y,k_x);$$

$$D_{55}(k_x,k_y)=D_{33}(-k_x,k_y);\quad D_{65}(k_x,k_y)=D_{43}(-k_x,-k_y);$$

$$D_{75}(k_x,k_y)=-D_{93}(-k_x,k_y);\quad D_{85}(k_x,k_y)=D_{83}(-k_x,k_y);$$

$$D_{95}(k_x,k_y)=-D_{73}(-k_x,k_y);\quad D_{10,5}(k_x,k_y)=-D_{83}(-k_x,-k_y);$$

$$D_{66}(k_x,k_y)=D_{33}(-k_y,k_x);\quad D_{76}(k_x,k_y)=D_{83}(-k_y,k_x);$$

$$D_{86}(k_x,k_y)=-D_{93}(-k_y,k_x);\quad D_{96}(k_x,k_y)=-D_{83}(-k_y,-k_x);$$

$$D_{10,6}(k_x,k_y)=-D_{73}(-k_y,k_x);\quad D_{10,7}(k_x,k_y)=-D_{87}(k_x,k_y);$$

$$D_{88}(k_x,k_y)=D_{77}(k_y,k_x);\quad D_{98}(k_x,k_y)=-D_{87}(k_y,-k_x);$$

$$D_{10,8}(k_x,k_y)=D_{97}(k_y,k_x);\quad D_{99}(k_x,k_y)=D_{77}(-k_x,k_y);$$

$$D_{10,9}(k_x,k_y)=D_{87}(-k_x,-k_y);\quad D_{10,10}(k_x,k_y)=D_{77}(-k_y,k_x).$$

The elements of the symmetrical array K are expressed as

$$K_{11}=K_{22}=K_{33}=K_{44}=K_{55}=K_{66}=1,$$

$$K_{77}=K_{88}=K_{99}=K_{10,10}=4L_2,$$

$$K_{31}=K_{51}=K_{42}=K_{62}=\frac{1}{2},$$

$$K_{53}=K_{64}=L_1,$$

$$K_{71}=-K_{91}=K_{82}=-K_{10,2}=-K_{73}=-K_{84}=K_{95}=K_{10,6}=L_2,$$

$$K_{75}=K_{86}=-K_{93}=-K_{10,4}=2L_2.$$

[1] J. G. Tobin, C. G. Olson, C. Gu *et al.*, Phys. Rev. B **45**, 5563 (1992).
[2] K. Gofron, J. C. Campuzano, H. Ding *et al.*, J. Phys. Chem. Sol. **54**, 1193 (1993).
[3] A. A. Abrikosov, J. C. Campuzano, and K. Gofron, Physica C **214**, 73 (1993).
[4] D. S. Dessau, Z.-X. Shen, D. M. King *et al.*, Phys. Rev. Lett. **71**, 2781 (1993).
[5] D. M. King, Z.-X. Shen, D. S. Dessau *et al.*, Phys. Rev. Lett. **73**, 3298 (1994).
[6] C. C. Tsuei, D. M. Newns, P. C. Pattnaik *et al.*, Phys. Rev. Lett. **65**, 2724 (1990).
[7] R. S. Markiewicz, J. Phys.: Cond. Matter **2**, 6223 (1990).
[8] D. M. Newns, P. C. Pattnaik, and C. C. Tsuei, Phys. Rev. B **43**, 3075 (1991).
[9] B. O. Wells, Z.-X. Shen, A. Matsuura *et al.*, Phys. Rev. Lett. **74**, 964 (1995).
[10] E. Dagotto, Rev. Mod. Phys. **66**, 763 (1994).
[11] W. Brenig, Phys. Rep. **251**, 4 (1995).
[12] V. J. Emery, Phys. Rev. Lett. **58**, 2794 (1987).
[13] C. M. Varma, S. Scmitt-Rink, and E. Abrahams, Sol. St. Commun. **62**, 681 (1987).
[14] C. E. Carneiro, M. J. De Oliveira, S. R. A. Salinas, and G. V. Uimin, Physica C **166**, 206 (1990).
[15] S. Trugman, Phys. Rev. B **37**, 1597 (1988).
[16] A. F. Barabanov, L. A. Maksimov, and G. V. Uimin, JETP Lett. **47**, 622 (1988); Zh. Éksp. Teor. Fiz. **96**, 665 (1989) [Sov. Phys. JETP **69**, 371 (1989)].
[17] J. R. Schrieffer, Phys. Rev. B **39**, 11663 (1989).
[18] A. F. Barabanov, R. O. Kuzian, and L. A. Maksimov, J. Phys.: Cond. Matter **3**, 9129 (1991).
[19] A. Nazarenko, K. J. E. Vos, S. Haas *et al.*, Phys. Rev. B **51**, 8676 (1995).
[20] O. A. Starykh, O. F. A. Bonfim, and G. F. Reiter, Phys. Rev. B **52**, 12534 (1995).
[21] D. Duffy and A. Moreo, Phys. Rev. B **52**, 15607 (1995).
[22] R. Hayn, A. F. Barabanov, J. Schulenburg, and J. Richter, Phys. Rev. B **53**, 11879 (1996).
[23] S. V. Lovtsov and V. Yu. Yushankhai, Physica C **179**, 159 (1991).
[24] M. Inui, S. Doniach, and M. Gabay, Phys. Rev. B **38**, 6631 (1988).
[25] A. Moreo, E. Dagotto, T. Jolicoeur, and J. Riera, Phys. Rev. B **42**, 6283 (1990).
[26] S. Bacci, E. Gagliano, and F. Nori, Int. J. Mod. Phys. B **5**, 325 (1991).
[27] A. F. Barabanov and V. M. Berezovskii, Zh. Éksp. Teor. Fiz. **106**, 1156 (1994) [JETP **79**, 627 (1994)]; J. Phys. Soc. Jap. **63**, 3974 (1994).
[28] H. Shimahara and S. Takada, J. Phys. Soc. Jap. **60**, 2394 (1991).
[29] A. F. Barabanov and O. A. Starykh, J. Phys. Soc. Jap. **61**, 704 (1992).
[30] A. F. Barabanov, V. M. Berezovsky, L. A. Maksimov, and E. Zhasinas, Physica C **252**, 308 (1995).
[31] E. B. Stechel and D. R. Jennison, Phys. Rev. B **38**, 4632, 8873 (1988).
[32] M. Ogata and H. Shiba, J. Phys. Soc. Jap. **57**, 3074 (1988).
[33] P. Prelovshek, Phys. Lett. A **126**, 287 (1988).
[34] J. Zaanen and A. M. Oles, Phys. Rev. B **37**, 9423 (1988).
[35] V. J. Emery and G. Reiter, Phys. Rev. B **38**, 4547 (1988).
[36] F. Mila, Phys. Rev. B **38**, 11358 (1988).
[37] M. S. Hybertsen, M. Shluter, and N. E. Christensen, Phys. Rev. B **39**, 9028, (1989).
[38] A. K. McMahan, J. F. Annett, and R. M. Martin, Phys. Rev. B **42**, 6268 (1990).
[39] F. C. Zhang and T. M. Rice, Phys. Rev. B **37**, 3759 (1988).
[40] H. Ding, G. Lang, and W. Goddard, Phys. Rev. B **46**, 14317 (1992).
[41] H. Mori, Prog. Theor. Phys. **33**, 423 (1965).
[42] H. Matsukava and H. Fukuyama, J. Phys. Soc. Jap. **58**, 2845 (1989).
[43] K. W. Becker, W. Brenig, and P. Fulde, Z. Phys. B **81**, 163 (1990).
[44] D. M. Frenkel, R. J. Gooding, B. I. Shraiman, and E. D. Siggia, Phys. Rev. B **41**, 350 (1990).
[45] A. F. Barabanov, L. A. Maksimov, and A. V. Mikheenkov, Sverkhprovodimost': Fizika, Khimiya, Tekhnologiya **4**, 3 (1991).
[46] G. Dopf, J. Wagner, P. Dieterich *et al.*, Phys. Rev. Lett. **68**, 2082 (1992).

[47]G. Dopf, A. Muramatsu, and W. Hanke, Phys. Rev. Lett. **68**, 353 (1992); Europhys. Lett. **17**, 559 (1992).
[48]R. Putz, R. Preuss, A. Muramatsu, and W. Hanke, Phys. Rev. B **53**, 5133 (1996).
[49]J. H. Jefferson, H. Eskes, and L. F. Feiner, Phys. Rev. B **45**, 7959 (1992).
[50]V. I. Belinicher and A. L. Chernyshev, Phys. Rev. B **49**, 9746 (1994).
[51]V. I. Belinicher, A. L. Chernyshev, and V. A. Shubin, Phys. Rev. B **53**, 335 (1996).

Note added in proof (6 September 1996). After the present work was submitted, Marshall *et al.* [D. S. Marshall, D. S. Dessau, A. G. Loeser *et al.*, Phys. Rev. Lett. **76**, 4841 (1996)] published an article in which and electronic structure evolution with hole doping in $Bi_2Sr_2Ca_{1-x}Dy_xCu_2O_{8+\delta}$ was investigated. The results of this work agree with our theory (compare our Figs. 2 and 3 and Figs. 3 and 4 from their investigation).

Translation was provided by the Russian Editorial office.